Evaluation and tuning of model trajectories and spreading rates in the Baltic Sea using surface-drifter observations

Joakim Kjellsson[1], Kristofer Döös[1], Tarmo Soomere[2],

[1] Department of Meteorology, Stockholm University, Sweden

[2] Laboratory of Wave Engineering, Institute of Cybernetics, Tallinn University of Technology, Estonia

August 31, 2012

Abstract

Results from surface-drifter experiments in the Baltic Sea in 2010-2011 are presented and discussed. The transport and spreading of the drifters are compared to results from model-simulated off-line trajectories. Differences between the observed and model-simulated trajectories are found for absolute dispersion (i.e. the distance travelled as a function of time) and relative dispersion (i.e. the distance between two initially paired trajectories as a function of time). The former is somewhat underestimated since the model-simulated currents are neither as fast nor as variable as those observed. The latter is underestimated both due to the above-mentioned reasons and due to the resolution of the ocean model.

The spreading rate of initially closely located water particles in the uppermost layer of thickness of about 1.5 m of the Gulf of Finland is studied using autonomous surface drifters. The average spreading rate increases with the increase in the time t elapsed from the deployment, equivalently, with the increase in the distance between drifters. The typical spreading rate is about 200 m day^{-1} for separations below 0.5 km, 500 m day^{-1} for separations below 1 km and in the range of 0.53 km day^{-1} for separations in the range of 14 km. The spreading rate does not follow the Richardsons law. The initial spreading, up to a distance of about $d = 100 - 150$ m,

is governed by the power law $d \sim t^{0.27}$ whereas for larger separations the distance increases as $d \sim t^{2.5}$.

1 Background

Many studies of the ocean rely on Lagrangian trajectories. Knowledge of the origin and destination of a water particle, as well as the spreading of several particles, is necessary for estimating the fate of oil spills (Soomere et al., 2010) or living organisms (Corell et al., 2011), as well as for planning rescues or finding lost goods. Trajectories can be either observed using drifters or floats, or simulated using a computer model of the ocean and a trajectory algorithm. Model-simulated trajectories may be used to track entire water masses (Döös, 1995; Blanke and Raynaud, 1997; Döös et al., 2004), or to map transport and dispersion in the ocean (Pizzigalli et al., 2007). As these studies become more frequent, the need for evaluating the model results against observations grow.

Several studies have used surface drifters or floats to validate model-simulated trajectories. These studies have covered *e.g.* the North Atlantic (Garraffo et al., 2001; McClean et al., 2002; Lumpkin et al., 2002), the Pacific (Garfield et al., 2001), and the world oceans (Döös et al., 2011). Although they employed different models, and different sets of Lagrangian observations, a common conclusion is that the distance travelled as a function of time (the absolute dispersion) show fair agreement between models and observations. Discrepancies between them are often found when studying the the separation between two initially paired trajectories (relative dispersion), and/or the variability of the currents (eddy kinetic energy). Relative dispersion and/or eddy kinetic energy is found too low in the models, thus the model-simulated trajectories do not separate as much as the observed ones. This can partly be attributed to the coarse resolution, which does not take turbulence on small scales into account, and implies a need for parameterizing sub-grid scale motions (Döös et al., 2011; Griffa et al., 2004).

For the Baltic Sea, there have been several studies using model-simulated trajectories (Döös et al., 2004; Soomere et al., 2010; Corell et al., 2011), but very little Lagrangian observational data. To the authors' knowledge, there has been only one surface-drifter experiment using SVP drifters as in this study (Håkansson and Rahm, 1993; Launiainen et al., 1993), and that drifter data has not been used to evaluate the accuracy of any ocean circulation model. This lack of observations can, at least partly, be explained by the small horizontal extent over which the mean depth exceeds the depth of the SVP-drifter drogue (18 m), and the the heavy traffic. The risk of a surface drifter getting caught up in too shallow waters or colliding with a ship is much higher in the Baltic Sea than in the world oceans.

A few short-term experiments have been performed in the Baltic Sea using drifters designed to follow the motions in the uppermost layer with a depth of $1-2$ m. In experiments in the Gulf of Finland (Gästgifvars et al., 2006) in May 2003 the buoys moved with a velocity of about 2% of the wind velocity and with a deviation angle of $0-10°$ to the right with respect to the local wind in moderate wind conditions. The behaviour of drifters was quite different in weak wind conditions: the currents were directed some 60° to the left of the wind apparently owing to the dynamics of the lower layers that overrode the local wind-induced drift. Similar experiments using drifters located in the uppermost 1 m layer were performed in 2007 in the Gulf of Finland to validate the output of the High Resolution Operational Model for the Baltic Sea (HIROMB) surface currents and to study dynamic ice drift (Kõuts et al., 2010). The duration of each deployment was up to 8 days in summer and a few months in ice conditions. Also, experiments targeted to the validation of the Seatrack Web oil fate model were performed with the same drifters in the middle of the Gulf of Finland, western Estonian archipelago and in the eastern sector of the northern Baltic Proper (Verjovkina et al., 2010). Their duration ranged from 8 hours up to 7 days. The longest distance covered during a single experiment was 52 nautical miles. Furthermore, an extensive analysis of the performance of six circulation models was also performed for the Gulf of Finland (Myrberg et al., 2010), and Soomere et al. (2010) highlighted systematic bias between modelled and measured wind direction and air flow properties in the central part of the Gulf of Finland.

On a larger scale, regional ocean models for the Baltic Sea have mostly been validated against data from moored instruments. Meier (2002) compared model-simulated profiles of temperature and salinity with observations from these stations and found fair agreement. It should, however, be noted that the number of observations was, and still is, quite small. The quality of the atmospheric forcing has also been assessed. (Höglund et al., 2009) showed that the probability distributions of observed wind speeds did not agree well to those from a regional atmospheric model used to compute the wind forcing. Generally, the model-simulated surface winds were found to be too low compared to observations along the Swedish coasts. For this reason, they utilized a gust correction to the model winds, which gave better results statistically, however for individual stations this deficiency can remain.

This study presents results from SVP surface drifters deployed in the Baltic Sea in 2010-2011. A wide range of statistics, such as mean net displacement and pair separations, have been calculated from the SVP-drifter data and the model-simulated trajectories, upon and the two data sets have been compared. Results from the comparison may then be used to tune the model-simulated trajectories to obtain a good fit to observations. The realism of the original and tuned model trajectories is discussed, as well as the implications for trajectory modelling in the Baltic Sea. Further on, we present results of a series of experiments with lightweight drifters in the Gulf of Finland that were designed to quantify the spreading of initially closely located floats owing to the dynamics of the uppermost $1-1.5$ m thick layer. Although the motion of such drifters was to some extent affected by surface-level wind, they apparently largely followed the currents.

2 Surface drifters in the Baltic Sea

12 SVP-B surface drifters (Lumpkin and Pazos, 2007) were deployed in the Baltic Sea in 2010-2011. The total period of data was 14 July 2010 - 19 November 2011. The drifters were manufactured by Marlin-Yug Ltd. in Sevastopol, Ukraine, and conform to internationally recognised standards, and are approved by NAVOCEANO (The Naval Oceanographic Office) to be of the WOCE (World Ocean Circulation Experiment) type. SVP-B drifters are equipped with a surface float containing GPS-sensors for measuring position, sea-surface temperature and atmospheric pressure, and a system to transmit the data to the Argos or Iridium satellites. Attached to the float is a holey sock between 12 and 18 meters depth. This allows for the drifters to follow sub-surface currents. Data – including the state of the drifter – are transmitted every hour. If, for some reason, the GPS gives an erroneous position, it can be, and was in our study, filtered out using positions estimated from the Argos or Iridium satellites.

The commonly-used SVP drifter used in this study is designed to represent currents at $12-18$ m depth with the wind- and wave-induced drift being negligible (Niiler et al., 1995; Pazan and Niiler, 2001). In most areas of the world oceans the depth of the upper mixed layer considerably exceeds this drogue depth. This is, however, not necessarily true for the Baltic Sea and especially in its semi-sheltered subbasins such as the Gulf of Finland, where the upper mixed layer is often less than 10 m thick (Leppäranta and Myrberg, 2009) and where the dynamics of the very thin surface and subsurface layers may be substantially decoupled from motions in the rest of the water column (Andrejev et al., 2004; Soomere et al., 2008). How a SVP drifter responds when some part of the drogue is in the mixed-layer, where wind forcing plays a large role, and some part is in the deeper layer below, where velocities generally are lower, is uncertain. Generally, the mixed layer is $15-20$ m deep in summer, and essentially none in winter (Meier, 2002).

Two pairs of SVP surface drifters were deployed in the Baltic Sea in July and August 2010. A triplet was then deployed at the same point in June 2011, and another triplet at a point to the northwest in August 2011. Two of the drifters from the two pairs stranded and were then re-deployed as a third pair in the Gulf of Finland in November 2011. All deployments, except the last pair, were made from the ferry M.S. Silja Festival on cruise between Stockholm and Riga.

Drifters of a different kind were deployed in the Gulf of Finland to study pair separations (Soomere et al., 2011). The active component (a high sensitivity (-159 dB) GPS/GSM device CT-24, Sanav Corp., Taiwan) of the lightweight floating buoys reported its position 4 times an hour. The device was mounted on the top of a 2 m long and 50 mm in diameter plastic pipe, about 2/3 of which was submerged and about 1/3 (60 cm) was above the water surface. Three deployments were made with altogether 8 drifters. Each time three drifters were deployed at a distance of about $50-150$ m from each other and let to drift from a few days to first weeks. Two deployments took place about 8 km west of the Island of Naissaar and one in Muuga Bay.

As a considerable part these shallow drifters was above water surface, their drift was impacted by wind properties to some extent. For example, the wind speed of 5 m/s may yield a contribution of about 10 cm/s to the drift speed (Soomere et al., 2011). Although this value is of the order of the current speed, its contribution to the changes in the distance between relatively closely located drifters apparently is not significant as the wind patterns over sea surface are much more homogeneous compared to similar winds over the mainland. Therefore, it is natural to expect that the impact of wind on closely located drifters mostly resulted in their concurrent downwind drift.

3 Model simulated trajectories

Model simulated trajectories were computed using the Lagrangian trajectory code TRACMASS (Döös, 1995; Blanke and Raynaud, 1997) driven by velocity fields from the Rossby Centre regional Ocean climate model (Meier et al., 2003). The RCO model is a coupled ice-ocean circulation model, and a regionalised version of the global OCCAM model (Webb et al., 1997). Here, the model grid covers the Baltic Sea with an open boundary at Kattegat. It is the ice-ocean component of the regional climate model RCAO (Döscher et al., 2002), to be used when predicting the future regional climate of Scandinavia. Several studies have validated RCO data against observations of temperature, sea surface height, and salinity. Meier (2002) used data from four separate stations in the Baltic Sea, and found that the model data agreed reasonably well. In our data set, RCO has been run separately, using observed river runoff. The atmospheric forcing is computed by downscaling ERA-40 fields (Uppala and co authors, 2005) to a smaller grid using the RCA (Kjellström et al., 2005). Data have subsequently been corrected to include some gustiness (Höglund et al., 2009). Ocean data, including temperature, salinity, and 3D velocity, were available every 6 hours with a 2 nm horizontal resolution and 41 model levels for the years 1961-2005.

TRACMASS trajectories are computed off-line, that is, after the fields from the RCO model have been integrated and stored. This allows for faster and less memory consuming computations. A thorough discussion of the pros and cons of the on-line and off-line methods of trajectory calculations is presented in Chapter 11. The model-simulated trajectories presently used were locked vertically, and horizontally driven by a weighted average of the currents between $12-18$ m. To simulate SVP drifters being stranded, any model drifter that at some point in time reached a depth shallower than 18 m is removed from the statistics.

TRACMASS includes tunable parameterisations of turbulence and diffusion to imitate sub-grid scale motions (Döös and Engqvist, 2007; Döös et al., 2011). The turbulence scheme adds a random increment to the velocity fields, while the diffusion scheme adds a random increment to the position. The random increment added by the turbulence scheme is proportional to the mass flux through the grid box, the time step, a random number, and a parameter A_H. The scheme is of low-order, meaning that it does not take into account such properties as Lagrangian time scales or Lagrangian velocity auto-correlation. This is often named as a "Markov 0" process (Rupolo, 2007).

4 Results

4.1 The surface drifters

The 12 surface drifters yielded equally many time series of data, however of very different length, where the mean drifter life time was $\sim$ 80 days (Table 1). For this reason, each drifter was split up into segments of $2^8 = 256$ hours. The power of 2 allowed for FFT calculations. This resulted in 85 segments for the data period which can be viewed as 85 independent drifters. Tracks of the surface drifters are shown in Figure 1. The full surface-drifter trajectories also resulted in 9 time series of pair separations (Fig. 2). It should be noted that the relative dispersion grew at very different rates. For instance, the pair "E1 & E2" dispersed rapidly after 5 days, while the pair "D1 & D3" stayed essentially paired for more than 20 days.

Velocities at each time step, except the last (eq. (3)), were calculated for each drifter (Fig. 4a). This showed strong currents near Poland, west of Estonia, and west of Gotland, regions were currents are known to be relatively strong. Subsequently, the Lagrangian time scales were computed using the velocity auto-correlations (eqs. (5) and (7)), yielding one time scale per drifter segment (Fig. 4b). As a short Lagrangian time scale indicates high flow variability, Fig. 4b highlights regions of higher eddy activity. Note that the time scales are similar to those calculated from SVP drifters in the world oceans (Rupolo, 2007).

Apart from the position, the surface drifters also collected data of sea-surface temperature (SST, Fig. 3) and atmospheric pressure. During summer-time temperatures reached $\sim 24°C$, while descending to near $0°C$ in winter. The one drifter lasting during the winter season always measured values above $0°C$, indicating ice-free conditions.

4.2 Model evaluation

36 model-simulated trajectories were started around the starting point of each surface drifter segment. Four of them originated in the same grid box as the surface drifter segment, while the others were spread horizontally in the eight adjacent grid boxes. Each grid box was about two nautical miles wide, which translates into a "cloud" of three nm ($\sim$ 6 km) radius of model trajectories around each surface-drifter segment. This took into account the variability around the starting point of each drifter, while the large number of model-simulated trajectories also resulted in clearer statistics. The years 2010-2011 were not available in our RCO data set, making anything but a statistical comparison impossible. The model trajectories were started in each available full model year, 1962-2004, at the same month, day, and hour as the surface-drifter segments. Furthermore, the drifter data in 2010-2011 were collected under ice-free conditions. However, the Baltic Proper and the Gulf of Finland may have been frozen during the winters of some of the years 1962-2004, in which case the effects on model-simulated trajectories are uncertain. For this reason, all segments during the period December 2010 - February 2011 were removed from the data, leaving only 76 drifter segments for the model evaluation. To resemble the surface drifters, the model-simulated trajectories were driven by the hori-

zontal velocities at $12 - 18$ m depth, with no vertical velocity. Only trajectories lasting for 256 hours without reaching waters shallower than 18 m were used.

The trajectory positions were stored every hour to have the same temporal resolution as the surface drifters. However, the velocity fields from the RCO model were only available every 6 hours. Hence, motions on time scales shorter than 12 hours were not resolved by the model, and time scales slightly longer were poorly resolved. The average velocity power spectrum of all surface drifter segments, and all model trajectories in each model year (Fig. 5, left), shows a peak near the frequency 2 cycles per day, corresponding to a period of ~ 14 hours. These are the inertial oscillations, and they are very pronounced for the surface drifters, and also visible for the model trajectories. However, for the model-simulated trajectories, there are two peaks. This is most likely an effect of the inertial oscillations being poorly resolved, leading to errors in the frequency. With a 14-hour running mean applied to the trajectory positions, the inertial oscillations were filtered out and the power spectra for the drifter data and model-simulated trajectories were comparable (Fig 5, right). This filter was applied to all calculations hereafter.

Absolute dispersion was calculated for the surface-drifter segments and the model trajectories (eq. (1)), and averaged over all drifter segments, and also over all model trajectories in each model year (Fig. 6). This mean absolute dispersion increased as a function of time, but generally started to level off after ~ 11 days, possibly to the small horizontal extent over which the depth is > 18 m in the Baltic Sea. The model-simulated trajectories trajectories in most model years were found to have lower absolute dispersion than the surface-drifter segments. To further investigate the differences in absolute dispersion, Fig. 7 shows the mean absolute dispersion after 256 hours for the surface drifter segments and all model years, with bars to indicate 90th and 10th percentiles. Apart from discrepancies in average absolute dispersion this also showed that the differences pertained also to the lowest and highest values of absolute dispersion (Fig. 6).

Hence, this indicates that the absolute dispersion of the surface drifters was systematically higher than that of the model trajectories. It is interesting to note that the 10th percentiles varied much less between model years than the 90th. The discrepancies between model results and observations in Fig. 7 indicates that the model-simulated velocities are lower than those observed. Indeed, the distribution of velocities for all drifter segments, and for all trajectories in each model year (Fig. 8) showed the latter to be narrower and centered over lower values than the former. These differences in velocity distributions can explain the differences in absolute dispersion.

Every trajectory has two Lagrangian velocity auto-correlations, one for zonal and one for meridional velocities. The total velocity auto-correlation is the average of the two. It was calculated and averaged over all surface-drifter segments and also over all model-simulated trajectories (eqs. 5-6) in each year (Fig. 9). It is necessary to point out that the velocity auto-correlation does not take the magnitude of the velocity into account, merely how it varies in time. A good agreement between model-simulated trajectories and surface-drifter segments was found only after the inertial oscillations had been filtered out. As shown before (Fig. 5), the observed and modelled trajectories resolve these motions very differently. The Lagrangian integral time scale, T_L, was calculated by integrating the auto-correlations (eq. (7)), where the lowest non-zero τ for which $R(\tau) = 0$ was used as upper limit of the integral (see Lumpkin et al. (2002) for comments on this, and other, methods). This was done for both zonal and meridional velocity auto-correlations, and the total Lagrangian integral time scale is defined as the average of the two time scales. Hence, there was one time scale for each trajectory. The distribution of T_L for the drifter data and for model-simulated trajectories in each model year is shown in Fig. 10. There is good agreement between the drifter data and corresponding model results, much attributable to the agreement in velocity auto-correlations.

Relative dispersion could not be calculated from the surface-drifter segments since the drifters need to be paired initially. For this reason, only the 12 complete drifter trajectories and the model-simulated trajectories originating from the starting point of these were used. As each of the surface-drifter pairs was simulated using $2 \cdot 36 = 72$ model trajectories, and each of the triplets using $3 \cdot 36 = 108$ model trajectories, this yielded 9 surface-drifter pairs, and > 5000 model pairs for each model year. The surface drifters were initially separated by $O(100\text{m})$, but the model-simulated trajectories had an initial separation of $O(100\text{m})-O(1000\text{m})$ as they were spread more widely around the surface drifter. Only pairs of initial separation < 1 km, thus $D_R(0) < 0.5$ km, were used for comparison. Averaged over all drifter pairs, and over all model-trajectory pairs for each model year, the relative dispersion was found much lower for the model trajectories than for the surface-drifter pairs (Fig. 11). Part of this difference may be due to the fact that the RCO model has a resolution of ~ 4 km and separation on smaller scales than that may not be resolved. To investigate this further, model-simulated trajectories initially separated by 4 to 12 km (approx. 1 to 3 grid boxes) were also compared to the surface-drifter pairs (Fig. 12). With a larger initial separation, the relative dispersion increased by an order of magnitude, however, it was still lower than that of surface drifter pairs. Furthermore, even though these pairs had model-trajectories in separate grid boxes, the rate of separation was lower than that of the surface drifters.

5 Tuning the trajectories

As previously noted, the model-simulated velocities were generally lower than those observed (Fig. 8). From Fig. 7 the mean drifter absolute dispersion is estimated to ~ 37 km, and the corresponding mean over all model years to ~ 30 km. This indicates that the model absolute dispersion is only $4/5$ of the observed. As a first approach, all model velocities were consequently multiplied by 1.25 and the simulations repeated. This resulted in mean absolute dispersion of the model trajectories shifted to values closer to that of the drifter segments

(Fig. 13), which would suggest that the model-simulated velocities were too low in the original simulation.

In another simulation, the turbulence scheme for TRACMASS, as introduced by Döös and Engqvist (2007) and Döös et al. (2011), was included. This adds extra velocity to the trajectories, but not necessarily in the same direction as that already present. The magnitude of the sub-grid turbulence is controlled by the parameter A_H, which was tuned to get values of mean absolute dispersion close to that of the drifter data. A fair fit was achieved for $A_H = 200$, close to the number used by Döös et al. (2011) for the world oceans, and results are shown in Fig. 13.

For both of the two above-mentioned methods, the distributions of Lagrangian integral time scales are shown in Fig. 14. The random motions introduced by the sub-grid turbulence shortened the Lagrangian integral time scales even though the data was filtered by a 14-hour running mean. This did not occur when the velocities were simply multiplied by the constant number 1.25 since that does not introduce any new motion, merely amplify that which is already present.

Relative dispersion was calculated from the new simulations and the results are shown in Fig. 15. Multiplying the velocities by a constant factor did not increase the relative dispersion significantly compared to Fig. 12. Adding sub-grid turbulence, however, resulted in an increase of both relative dispersion and separation rate, with values closer to those of the drifter data. For the initially close trajectories ($D_R(0) < 0.5$km), adding the sub-grid turbulence resulted in good agreement at times > 10 days. It ought to be noted that the magnitude of the sub-grid parameterisation is chosen to give a good fit for absolute dispersion, not relative dispersion.

6 Spreading rate in the Gulf of Finland

The spreading rate of initially closely located water particles, passive drifters or floats in the surface layer of the Gulf of Finland was studied using autonomous surface drifters located in the uppermost layer with a depth of about 1.5 m (Soomere et al., 2011). The state-of-the-art 3D circulation models adequately replicate the major features of the hydrophysical fields of natural water bodies. The limited resolution of the models in time and space usually does not significantly affect the statistical properties of the basic hydrographical fields such as temperature, salinity or density but may substantially modify the statistical properties of the drift of various substances due to the impact of small-scale motions (frequently called sub-grid turbulence because it is not explicitly accounted for in the model). The standard way to circumvent this difficulty is to use ensembles of models for trajectory simulations (Vandenbulcke et al., 2009), to "shake" the trajectories as described above, or to rely on statistical analysis of large pools of simulations of the drift and transport patterns (Soomere et al., 2010, 2011). The latter approach, extensively used in the following chapters, generally requires accounting for the processes of (local) turbulent spreading that tend to separate initially closely positioned drifters (otherwise the modelled particles released in a single grid cell will drift together for a long time). The correct parameterization of subgrid-scale processes is a challenge in water bodies such as the Gulf of Finland that are extremly strongly stratified and have very small baroclinic Rossby radius (usually $2-4$ km, (Alenius et al., 2003)). In such relatively shallow basins it is not clear beforehand whether the spreading of surface floats is governed by velocity fluctuations in a relatively thick surface layer or by the dynamics of the uppermost layer.

The primary measure of spreading is the rate of increase in the distance of initially closely located water particles (equivalently, passive drifters). This rate can be approximated by a power function or an exponential law of the time t elapsed from the release of the particles. The classical notion for the average distance between two particles in a turbulent velocity field, the Richardsons law (Richardson, 1926) applies in fully developed 3D turbulent flows where the average difference between velocity fluctuations $\mathbf{v}(\mathbf{r},t)$ follows the (Kolmogorov) power law $\langle|\mathbf{v}(\mathbf{r},t)-\mathbf{v}(\mathbf{r}+\mathbf{\Delta r},t)|\rangle = A\,|\Delta\mathbf{r}|^a$ (Falkovich et al., 2001). Here angle brackets denote averaging over the coordinate $\mathbf{r}$ and/or over the ensemble of flows, A is a constant and the exponent $a = 1/3$ is specific to the fully developed 3D turbulent flow. In such an environment, the average distance d between a pair of tracers scales as $d \propto t^b$, where $b = 1/(1-a)$. In the case of the Kolmogorov law $a = 1/3$, the corresponding exponent is $b = 3/2$. The above-discussed relative dispersion D^2 and the relevant diffusivity coefficient can be obtained as $D^2(t) = \left\langle d^2(t)\right\rangle$ (Lumpkin and Elipot, 2010).

The character of spreading is essentially different in 2D flows where at scales smaller than the energy input scale, the velocity spectrum is dominated by the enstrophy cascade and $a = 1$. The exponent $b \to \infty$ and an exponential growth of the distance with time (the Lins law) occurs (Lin, 1972; Falkovich et al., 2001; LaCasce, 2008). Thus, for an ideal 2D turbulence with a single energy input scale λ, while the Lins law is expected to be valid for scales below λ whereas Richardsons law is related to large-scale circulation (Salazar and Collins, 2009). Both these flow regimes have been observed in the open ocean (Ollitrault et al., 2005) and in the Baltic Sea for different scales (Döös and Engqvist, 2007).

Contrary to the above-mentioned theoretical expectation, the Richardsons law seems to fairly well describe spreading properties for small distances whereas the Lins law shows a better fit for large distances (Döös and Engqvist, 2007). A probably reason for this counter-intuitive observation is that the character of spreading is particularly complicated for 2D flows occurring on the surface of 3D flows, which is often the case in strongly stratified environments. Such flows may be highly compressible[1] and may exhibit a considerable decrease in

[1] The (flow) compressibility is defined as the relative weight of the potential component in the decomposition of the net velocity field into solenoidal and potential components.

b compared to the pure 2D case (Bec et al., 2004; Kalda, 2007). For a review of relevant laboratory experiments see Cressman et al. (2004). For realistic geophysical flows one might expect quite a large variation $1.5 \leq b < \infty$ of this exponent.

Soomere et al. (2011) presented results of an attempt to experimentally estimate the resulting finite value of the exponent b in the uppermost layer of the Gulf of Finland, the motions in which are responsible for a large part of the pollution transport. Differently from above and from a number of similar earlier studies (Ollitrault et al., 2005; Döös and Engqvist, 2007; Lumpkin and Elipot, 2010) the experiments performed in the western and central part of the Gulf of Finland in August-October 2010 were concentrated on relatively small initial distances of the drifters ($\sim$ 100 m). The system of currents in the Gulf of Finland reveals a complicated pattern of basin-scale mostly cyclonic circulation, optionally anticyclonic gyre in the surface layer in the eastern part of the gulf (Soomere et al., 2011), exchange of water masses with the Baltic Proper, a variety of meso-scale synoptic eddies and frequent 3D effects (see Chapter 3 for more detailed information). The contemporary circulation models for the Gulf of Finland have a spatial resolution of about 2 nautical miles (3.7 km) (Myrberg et al., 2010; Andrejev et al., 2011) or better. Therefore, it is reasonable to assume that at scales larger than about $4-5$ km both the spreading and transport properties are reasonably resolved by the majority of the models of the Gulf of Finland. For this reason, we focus on spreading properties driven by small-scale features up to distances of a few kilometres between the drifters.

The deployments resulted in 7 pairs of drifter trajectories. As the signal from the drifters was at times lost, it was not possible to adequately calculate the detailed statistics of the drift but the recorded data still allowed quantification of the temporal evolution of the separation of the counterparts. The observed trajectories reflected a variety of phenomena characteristic to the current field of the Gulf of Finland (Fig. 16): the presence of relatively small meso-scale eddies with a diameter of about 5 km to the north of Naissaar, inertial oscillations in the open part of the gulf, and relatively rapid almost straight drift sections (cf. Kõuts et al. (2010),Verjovkina et al. (2010)). While most of the trajectories were relatively short (below 50 km), one alongshore drifting device covered more than 150 km during about two weeks and left the Gulf of Finland to the Baltic Proper.

The emphasis in Soomere et al. (2011) was on the relationship between the measured distance d between drifters in pairs and the rate of increase (spreading rate) in this distance. The spreading rate depends heavily on the time t elapsed from deployment and, therefore, on the instantaneous distance between the drifters. The typical spreading rate was almost constant for all the pairs within the first $10-15$ hours until the drifters were separated by about 150 m and increased considerably afterwards (Fig. 17). Although the estimates for initial distances below 100 m should be interpreted as indicative because of possible uncertainties of GPS-measured locations, such a behaviour suggests the presence of different regimes of spreading (either ballistic or Richardsons law) for initially closely located drifters up to separations of about 150 m. The spreading rate owing to the impact of basically random component of marine turbulence (also called random walk regime, Lumpkin and Elipot (2010)) can be estimated from the initial sections (the parts that reveal no extensive quasi-periodic variations due to coherent structures) of the drifters motion in Fig. 17. This rate is about $200-300$ m/day, that is, about twice as large as hypothesised in Andrejev et al. (2010).

For drifters initially separated by less than 1 km this rate varied from about 100 m/day to 700 m/day. For even larger distances between the drifters (>600 m) it revealed somewhat different behaviour for different pairs. The distance persistently increased for several pairs but revealed quasi-regular oscillations for some other pairs. This phenomen is probably common for the Gulf of Finland (cf. Verjovkina et al. (2010)) and is apparently caused by relatively small meso-scale eddies with a diameter as small as about 400 m.

7 Power law representation of the spreading rate

The presented data suggests that the structure of small-scale turbulence in the study area may contain motions of substantially different character at different scales. The substantial decrease in the average spreading rate for distances of $1.6-3.2$ km during a certain time interval (Fig. 17) is apparently owing to a substantial impact from meso-scale eddies with a diameter matching the local Rossby radius that, ideally, should be resolved by the hydrodynamic model.

It is interesting to analyse whether the dynamics of the study site is mostly governed by 3D (local) turbulence or by 2D (large-scale) motion system. The distance between the drifters increased approximately linearly in the linear power law $2/3$ (corresponding to the theoretical spreading rate for the 3D turbulence) coordinates only until values of about 400 m (equivalently, during about 25 hours), after which the separation rate started to increase for the majority of pairs. Remarkably, two pairs revealed linear separation in this framework and thus an almost perfect match with the properties of the 3D turbulence after $2-2.5$ days of drifting. The distance between the drifters was more than 4 km, a scale which is usually resolved by the contemporary circulation models. The relevant drifters were deployed on 12 August 2010 in relatively calm weather conditions and thus were only weakly, if at all, impacted by the wind.

The above suggests that there probably exists no single proper fit of the exponent b in the power law $d \sim t^b$. This is confirmed by the analysis in log-log coordinates (Fig. 19). For relatively small separations (below 70 m in the initial phase of the drift, up to 8 hours) the exponent b was in the range $0.23-0.3$, with a mean value of 0.27. Therefore, the separation rate is governed by a ballistic law rather than the Richardsons law. As none of these laws dominated, certain specific mechanisms, such as shear dispersion (particle separation due to variation of the mean velocity field) or specific surface-layer dispersion (induced by the gradient of the energy dissipation rate in the turbulent surface layer (Skvortsov et al., 2010), may govern the initial particle separation rate.

Starting from a separation of about 100 m (or a drift time of 10 hours), this increase occurred much faster. Two pairs in Fig. 19 evidently were involved into coherent motions. This is reflected by the best fit for the exponent $b = 1.3$ and $b = 0.88$ for these pairs. All other pairs revealed surprising match of the spreading rates. The exponent b for them varied from 2.12 to 2.72, with the average value of $b \approx 2.5$. A regression analysis of the dependence of the average distance on the drift time led to a fairly similar result if all the pairs are involved or $b \approx 2.5$ if the above two pairs are excluded. Both the resulting values are of a reasonable magnitude compared to the infinite exponent characterising 2D flows but yet clearly larger then the classical Richardsons value $b = 1.5$ characteristic to the 3D turbulent motions. Therefore, in the study area the dynamics was predominantly governed by 3D flows but the contribution of a 2D motion system, apparently present in the surface layer, was still substantial.

8 Discussion and Conclusions

Results from recent deployments of surface drifters in the Baltic Sea during the summers of 2010 and 2011 have been presented. Two types of drifters were used; the SVP drifters have a 18 m drogue depth and represent motions between $12-18$ m depth, while the other drifters are much more shallow and thus represent only the uppermost $1-1.5$ m currents. The average life time of a SVP surface drifter was 80 days. These drifters have been used to map some geographical aspects of the sub-surface currents in the Baltic Proper (Fig. 4a), and to obtain values of net displacement and dispersion as a function of time (Figs. 6 and 12). The SVP surface drifters were split up into segments of ~ 11 days each, and the segments were compared to model-simulated trajectories starting at the same position and time as the drifter segments. In order to remove inertial oscillations, which were well observed in the drifter data but not very well in the ocean circulation model, all drifter segments and model-simulated trajectories were filtered using a 14-hour running mean. As ocean model data was not available for 2010 and 2011, the drifter segments had to be compared to model-simulated trajectories in the years available, 1962-2004. As such, the motion of a drifter segment could not be compared to any specific model-simulated trajectory. However, some indications follow from a statistical comparison. It must be stressed that the years 2010-2011 could have been "extreme" events in terms of absolute dispersion. From Fig 7, it is noted that such events are quite uncommon, and the likelihood that they would occur over a two-year period is thus even smaller.

The absolute dispersion was found to be significantly lower for the model trajectories than for the observed drifters. This was attributed to the model velocities being lower and less variable, as shown by comparing the PDF of Lagrangian velocities from drifters to that of the model trajectories. Near-surface currents are, to some extent, wind-driven on time scales comparable to the duration of the drifter segments (Leppäranta and Myrberg, 2009). The quality of model-simulated near-surface currents thus depends on the quality of the wind forcing, mixed-layer depth, and parameterization. Meier (2002) compared RCO temperature and salinity profiles to observations and found good agreement in mixed-layer depth. The wind forcing (ERA-40 winds, dynamically downscaled by the RCA model), on the other hand, was corrected by Höglund et al. (2009) using a parameterisation of wind gusts, as the wind speeds were found not to be variable enough. The correction yielded somewhat more realistic frequency distributions of the wind speeds. However, this does not imply that the wind at a specific point or time became more realistic. R.M.S. errors may very well have increased with this correction. Furthermore, the study was limited to the Swedish coastal regions, as no observations over open water were available. Thus, there is no information about the quality of the wind forcing over open water, although it is likely to share some of the problems of the coastal winds. It is thus conceivable that any errors in the near-surface currents, to a large part, are due to errors in the wind field from RCA.

Multiplying the velocities in RCO by a factor 1.25 or including parameterised sub-grid turbulence resulted in better agreement to observed velocities and absolute dispersion for the model-simulated trajectories. Although both methods yielded similar results for absolute dispersion, the results were very different when investigating other metrics. The Lagrangian integral time was severely shortened when adding sub-grid turbulence, resulting in time scales shorter than those of the drifter segments. The random motions introduced when adding the turbulence parameterisation (Döös et al., 2011) do not take the original velocity into account, thus changing the both the velocity and properties of the trajectory somewhat. The transport speed can thus be improved with this parameterisation, but at the cost of changes in *e.g.* direction. To tune the model trajectories for single-particle statistics, multiplying the model-simulated velocities by a constant factor would then be a better choice of method, as it increases the speed but does not alter the properties of the trajectory. When tuning model trajectories to relative dispersion this is, however, a poor choice since small, sub-grid scale changes in direction is what is needed to separate initially paired model trajectories. Furthermore, even for model-simulated trajectories separated by at least one grid box, the separation rates were lower than the surface-drifter average, implying that sub-grid parameterisation is needed also on larger scales ($> 4km$).

Using values roughly estimated from Fig. 7 and Fig. 11, some implications for trajectory modelling without tuning can be identified. If the model-simulated trajectories have 4/5 of the absolute dispersion of the drifter segments, this would mean that if model trajectories, on average, travel 100 km in 10 days, a drifter, or a real water particle, would, on average travel 125 km in those 10 days. By the same argument, if model trajectories are estimated to reach the coast in 10 days, real water particles would make the same journey in 8 days. Furthermore, water particles contained within a < 1 km radius initially would spread over an area of 12 km radius in 25 days, while their model counterparts would spread to cover < 2 km radius. Such conclusions would have impacts when estimating the fate of oil-spills or other pollutants. However, we wish to stress that we have compared observations from 2010-2011 with model data from 1962-2004, and that the drifter data is limited.

To make the model-observation comparison fair, and to yield more confidence in the magnitudes of the tuning needed would require model data for the years 2010-2011. This could, however, take a few years as the RCO model is being decommissioned in favour for a new regional ocean model, based on the NEMO ocean circulation model (Madec, 2008). The wind forcing will most likely also need updating, as the ERA-40 data set is to be replaced by ERA-Interim and eventually by ERA-75, while the RCA model is also likely to be decommissioned. If surface drifter data is continued to be gathered for the Baltic Sea, this data could be used to validate and perhaps tune the next generation of Baltic Sea models.

The presented results from the shallowest drifters indicate substantial difference in the dynamics of the vertically integrated relatively thick layer and the uppermost layer with a thickness of $1 - 1.5$ m. On the one hand, understanding of the rules governing the former dynamics are essential for the transport of large water masses, substantial amounts of nutrients, dissolved chemicals etc. that are distributed over a surface layer of considerable thickness and/or are able to move between different layers in the euphotic zone (fish larvae, different algae, etc.). On the other hand, the laws governing the trajectories and fate of objects and substances in the uppermost thin water sheet are evidently decisive for substances and objects of slightly positive buoyancy such as lighter fractions of oil, floats, plastic debris, lost containers, etc.

The parameters characterising the dynamics of spreading of objects in the uppermost layer are of utmost importance for the technique developed in this book. Its key idea is to use the Lagrangian dynamics of currents to develop methods for the reduction of environmental risks. Its key component is statistical analysis of large sets of Lagrangian trajectories of virtual drifters or water particles. These statistics are evidently highly sensitive with respect to the parameterisation of subgrid-scale processes that may randomly redirect drifters to largely different sea areas compared to the modelled fields of currents (Döös, 1995; de Vries and Döös, 2001; Griffa et al., 2004; Andrejev et al., 2010). The problem is even more complicated in strongly stratified sea areas such as the Gulf of Finland where the drift is frequently steered by multi-layered dynamics (Andrejev et al., 2004; Gästgifvars et al., 2006) and where it is not clear beforehand which theoretical framework (predomination of 2D or 3D motion systems) should be used in the analysis. Similar problems intrinsically arise in the attempts of modelling of pathways of different water masses (Meier, 2007) and especially in simulations, both in forecast and hindcast modes, of pollution transport by 3D hydrodynamic models such as HIROMB or Seatrack Web (Funkquist, 2001; Gästgifvars et al., 2006; Verjovkina et al., 2010).

Although the average spreading rate generally increases with the increase in the time or the distance between drifters, the well-known Richardsons law does not become evident for the transport in the uppermost layer of the Gulf of Finland. The initial evolution of closely located drifters to some extent resembles the ballistic law but a power law $d \sim t^{0.27}$ much better describes the spreading in the range of distances from the first tens of meters up to about $100 - 150$ m. Starting from this threshold, the distance increases, in average, according to a power law $d \sim t^{2.5}$. The typical spreading rate is about 200 m/day for separations below 0.5 km, 500 m/day for separations below 1 km and in the range of $0.5 - 3$ km/day for separations in the range of $1 - 4$ km.

The results suggest that a realistic parameterization of sub-grid-scale processes in the Gulf of Finland strongly depends on the resolution of the ocean model. Models with spatial resolution coarser than 2 km apparently cannot resolve meso-scale dynamics in this region. If they are used by some reason, the parameterization of subgrid-scale processes should correspond to a typical spreading rate of about 2 km/day. The same rate is reasonable for models with a resolution of about $1-2$ km while the models with a resolution of ~ 1 km might use the rate of about 700 m/day. Parameterisations leading to spreading rates of $300-500$ m/day may be recommended for extremely high-resolution models with a grid step of ~ 0.5 km. As the drifters in the uppermost layer have experienced a certain impact of the local wind and waves on their drift the presented rates may to some extent overestimate the actual spreading rates but the order of magnitude for the spreading effects extracted from the experiments evidently is realistic.

A Lagrangian statistics

The absolute dispersion is a measure of the net displacement from the origin as a function of time. Averaged over M trajectories, it is defined as

$$D_n \equiv \sqrt{\frac{1}{M}\sum_{m=1}^{M}\sum_{i=1}^{2}\left(x_{i,m,n}-x_{i,m,0}\right)^2}, \tag{1}$$

where n is the time step, m is the trajectory, and i is the dimension.

Relative dispersion is often defined as the distance from the mean position at a certain time. However, here it is defined as half the pair separation, *i.e* half the distance between two trajectories at a given time step. The two definition are essentially equivalent, however, relative dispersion yields one value per trajectory and time step while pair separation yields one value per pair and time step. With the same notations as for the absolute dispersion, the average over P pairs is defined as

$$D_R(t) \equiv \sqrt{\frac{1}{P}\sum_{p=1}^{P}\sum_{i=1}^{2}[x_{i,q}(t)-x_{i,r}(t)]^2}, \tag{2}$$

where p is the particle pair consisting of trajectories r and q. The square of the separation ensures positive values.

The Lagrangian velocity is obtained by using a non-centered finite difference.

$$v_i(t) \equiv \frac{dx_i(t)}{dt} \approx v_{i,n} \equiv \frac{x_{i,m,n} - x_{i,m,n-1}}{t_n - t_{n-1}}, \tag{3}$$

with the same indices as before. Similarly, the acceleration was calculated by finite differencing the velocity.

$$a_i(t) \equiv \frac{dv_i(t)}{dt} \approx a_{i,n} \equiv \frac{v_{i,m,n} - v_{i,m,n-1}}{t_n - t_{n-1}}. \tag{4}$$

Note how velocity is not defined at the first position, and acceleration is not defined at the first velocity.

The Lagrangian velocity auto-correlation describes the correlation of the velocity at one time with that of previous times. The definition is

$$R_q = \frac{\sigma_q^2}{\sigma_0^2}, \tag{5}$$

where σ_q^2 and σ_0^2 are the Lagrangian velocity auto-covariances for time lag q and no lag respectively. σ_q^2 is defined as

$$\sigma^2(\tau) = \lim_{T\to\infty} \frac{1}{T} \int_0^T \mathbf{u}'(t+\tau) \cdot \mathbf{u}'(t)\ dt \approx \sigma_q^2 \equiv \sum_{i=1}^{2} \frac{1}{N-q-1} \sum_{n=1}^{N-q-1} u'_{i,n} u'_{i,n+q}, \tag{6}$$

where $u'_{i,n} = u_{i,n} - \overline{u}_i$ and $\overline{u}_i$ is a time average of the segment.

Using the autocorrelation, $R(\tau)$, the Lagrangian integral time scale, T_L is defined as,

$$T_L = \int_0^\infty R(\tau)\ d\tau. \tag{7}$$

This is a measure of the *memory* of a trajectory, that is, the time lag during which the Lagrangian velocity is correlated. When computing this integral, the point where $R(\tau) = 0$ for the first time is used here as upper bound. This truncation is perhaps the most commonly used, due to the noisy character of the auto-correlation function, $R(\tau)$, for large τ. Lumpkin et al. (2002) compared this approximation with several other approximations, and found that all of them produced essentially the same results, thus concluding that the approximation used here is a robust one.

Acknowledgements

This study was performed in the framework of the BONUS+ project BalticWay (financed by the BONUS EEIG). This study was performed in the framework of the BalticWay project, which is supported by the funding from the European Communitys Seventh Framework Programme (FP/20072013) under grant agreement No. 217246 made with the joint Baltic Sea research and development programme BONUS. The research was partially supported by the Estonian Science Foundation (grant No 9125), targeted financing by the Estonian Ministry of Education and Research (grant SF0140007s11), and by the European Regional Development Fund via support to the Centre of Excellence for Non-linear Studies CENS. The authors wish to thank Tallink-Silja shipping company for authorising us to deploy the surface drifters from the Stockholm-Riga line and in particular we wish to thank Captain Lembit Uustulnd and his crew on M/S Silja Festival for permission and help in deployment of the surface drifters. We also acknowledge and appreciate the help given by Prof. Peter Lundberg and Dr. Anders Engqvist in deployment. Experiments with the surface drifters in the Gulf of Finland were performed very professionally by Mr Mikk Viidebaum. His cooperation towards deployment and rescue of subsurface drifters is also gratefully acknowledged. Finally, we also extend gratitude to Markus Meier and Anders Höglund at SMHI for providing RCO data as well as help and fruitful discussions about it. All trajectory simulations have been made using supercomputers maintained by NSC at Linköping University, Sweden.

References

Alenius, P., A. Nekrasov, and K. Myrberg, 2003: The baroclinic rossby-radius in the gulf of finland. *Continental Shelf Research*, **23**, 563–573.

Andrejev, O., K. Myrberg, P. Alenius, and P. A. Lundberg, 2004: Mean circulation and water exchange in the gulf of finland - a study based on three-dimensional modelling. *Bor. Env. Res.*, **9**, 1–16.

Andrejev, O., A. Sokolov, T. Soomere, R. Värv, and B. Viikmäe, 2010: The use of high-resolution bathymetry for circulation modelling in the gulf of finland. *Estonian Journal of Engineering*, **16**, 187–210.

Andrejev, O., T. Soomere, A. Sokolov, and K. Myrberg, 2011: The role of spatial resolution of a three-dimensional hydrodynamic model for marine transport risk assessment. *Oceanologia*, **53(1-TI)**, 309–334.

Bec, J., K. Gawedzki, and P. Horvai, 2004: Multifractal clustering in compressible flows. *Physical Review Letters*, **92(22):224501**.

Blanke, B. and S. Raynaud, 1997: Kinematics of the pacific equatorial undercurrent: An eulerian and lagrangian approach from gcm results. *J. Phys. Oceanogr.*, **27**, 1038–1053.

Corell, H., P. Moksnes, A. Engqvist, K. Döös, and P. Jonsson, 2011: Larval depth distribution critically affects dispersal distance and optimum size for marine protected areas. *Submitted to Marine Ecology Progress Series.*

Cressman, J., J. Davoudi, W. Goldburg, and J. Schumacher, 2004: Eulerian and lagrangian studies in surface flow turbulence. *New Journal of Physics*, **6**, 53.

de Vries, P. and K. Döös, 2001: Calculating lagrangian trajectories using time-dependent velocity fields. *J. Atmos. Ocean Tech.*, **18**, 1092–1101.

Döös, K., 1995: Interocean exchange of water masses. *J. Geophys. Res.*, **100**, 13499–13514.

Döös, K. and A. Engqvist, 2007: Assessment of water exchange between a discharge region and the open sea - a comparison of different methodological concepts. *Estuarine, Coastal and Shelf Science*, **74**, 585–597.

Döös, K., H. E. M. Meier, and R. Döscher, 2004: The baltic haline conveyor belt or the overturning circulation and mixing in the baltic. *Ambio*, **33**, 261–266.

Döös, K., V. Rupolo, and L. Brodeau, 2011: Dispersion of surface drifters and model-simulated trajectories. *Ocean Modeling*, **39**, 301–310.

Döscher, R., U. Willén, C. Jones, A. Rutgersson, H. E. M. Meier, U. Hansson, and L. P. Graham, 2002: The development of the regional coupled ocean-atmosphere model rcao. *Bor. Env. Res.*, **7**, 183–192.

Falkovich, G., K. Gawedzki, and M. Vergassola, 2001: Particles and fields in fluid turbulence. *Reviews in Modern Physics*, **73(4)**, 913–975.

Funkquist, L., 2001: Hiromb, an operational eddy-resolving model for the baltic sea. *Bulletin of the Maritime Institute in Gdańsk*, **28**, 7–16.

Garfield, N., M. Maltrud, C. Collins, T. Rago, and R. Paquette, 2001: Lagrangian flow in the california undercurrent, an observation and model comparison. *J. Mar. Sys.*, **29**, 201–220.

Garraffo, Z. D., A. J. Mariano, G. A., C. Veneziani, and E. P. Chassignet, 2001: Lagrangian data in a high-resolution numerical simulation of the north atlantic 1 - comparison with in situ drifter data. *J. Mar. Sys.*, **29**, 157–176.

Gästgifvars, M., H. Lauri, A.-K. Sarkanen, K. Myrberg, O. Andrejev, and C. Ambjörn, 2006: Modelling surface drifting of buoys during a rapidly-moving weather front in the gulf of finland, baltic sea. *Estuarine, Coastal and Shelf Science*, **70**, 567–576.

Griffa, A., L. Piterbarg, and T. Özgökmen, 2004: Predictability of lagrangian particle trajectories: Effects of smoothing of the underlying eulerian flow. *J. Mar. Res.*, **62**, 1–35.

Håkansson, B. and L. Rahm, 1993: Swedish lagrangian current experiments. In *Gulf of Bothnia Year 1991 - Physical Transport Experiments*, volume 15. SMHI, RO, 41–55.

Höglund, A., H. Meier, B. Broman, and E. Kriezi, 2009: *Validation and correction of regionalised ERA-40 wind fields over the Baltic Sea using the Rossby Centre Atmosphere model RCA3.0*. Swedish Meteorological and Hydrological Institute, SE-601 76, Norrköping, Sweden.

Kalda, J., 2007: Sticky particles in compressible flows: Aggregation and richardson's law. *Physical Review Letters*, **98(6):064501**.

Kjellström, E., L. Bärring, S. Gollvik, U. Hansson, C. Jones, P. Samuelsson, M. Rummukainen, A. Ullerstig, U. Willén, and K. Wyser, 2005: A 140-year simulation of european climate with the new version of the rossby centre regional atmospheric climate model (rca3). *Reports Meteorology and Climatology*, **108**.

Kõuts, T., S. Verjovkina, P. Lagemaa, and R. U, 2010: Use of lightweight on-line gps drifters for surface current and ice drift observations. In *2010 IEEE/OES US/EU Baltic International Symposium, August 25–27, 2010, Riga, Latvia, IEEE*, 10.

LaCasce, J., 2008: Statistics from lagrangian observations. *Progress in Oceanography*, **77**, 1–29.

Launiainen, J., T. Stipa, H. Grönwall, and T. Vihma, 1993: Finnish lagrangian current experiments. In *Gulf of Bothnia Year 1991 - Physical Transport Experiments*, volume 15. SMHI, RO, 55–67.

Leppäranta, M. and K. Myrberg, 2009: *Physical Oceanography of the Baltic Sea*. Springer-Praxis, Berlin.

Lin, J. T., 1972: Relative dispersion in the enstrophy-cascading inertial range of homogeneous two-dimensional turbulence. *J. Atmos. Sci.*, **29**, 394–396.

Lumpkin, R. and S. Elipot, 2010: Surface drifter pair spreading in the north atlantic. *J. Geophys. Res.*, **115**(C12017).

Lumpkin, R. and M. Pazos, 2007: *Lagrangian analysis and prediction of coastal and ocean dynamics*. Cambridge University Press, New York.

Lumpkin, R., A.-M. Treguier, and K. Speer, 2002: Lagrangian eddy scales in the northern atlantic ocean. *J. Phys. Oceanogr.*, **32**, 2425–2440.

Madec, G., 2008: Nemo ocean engine. *Note du Pole de modélisation*, **27**.

McClean, J. L., P.-M. Poulain, J. Pelton, and M. E. Maltrud, 2002: Eulerian and lagrangian statistics from surface drifters and a high-resolution pop simulation in the north atlantic. *J. Phys. Oceanogr.*, **32**, 2472–2491.

Meier, H., 2002: Regional ocean climate simulations with a 3d ice-ocean model for the baltic sea. part 1: Model experiments and results for temperature and salinity. *Clim. Dyn.*, **19**, 237–253.

Meier, H., R. Döscher, and T. Faxén, 2003: A multiprocessor couple ice-ocean model for the baltic sea: Application to salt inflow. *J. Geophys. Res.*, **108**(C8).

Meier, H. E. M., 2007: Modeling the pathways and ages of inflowing salt- and freshwater in the baltic sea. *Estuarine, Coastal and Shelf Science*, **74**, 610–627.

Myrberg, K., V. Ryabchenko, A. Isaev, R. Vankevich, O. Andrejev, J. Bendtsen, A. Erichsen, L. Funkquist, A. Inkala, I. Neelov, K. Rasmus, M. Rodriguez Medina, U. Raudsepp, J. Passenko, J. Söderkvist, A. Sokolov, H. Kuosa, T. R. Anderson, A. Lehmann, and M. D. Skogen, 2010: Validation of three-dimensional hydrodynamic models in the gulf of finland based on a statistical analysis of a six-model ensemble. *Bor. Env. Res.*, **15**, 453–479.

Niiler, P. P., A. S. Sybrandy, B. Kenong, P. M. Poulain, and D. Bitterman, 1995: Measurements of the water-following capability of holey-sock and tristar drifters. *Deep-Sea Res.*, **42**, 1951–1964.

Ollitrault, M., C. Gabillet, and A. Colin de Verdiere, 2005: Open ocean regimes of relative dispersion. *Journal of Fluid Mechanics*, **533**, 381–407.

Pazan, S. E. and P. P. Niiler, 2001: Recovery of near-surface velocity from undrogued drifters. *J. Atmos. Ocean Tech.*, **18**, 476–489.

Pizzigalli, C., V. Rupolo, E. Lombardi, and B. Blanke, 2007: Seasonal probability dispersion maps in the mediterranean sea obtained from the mediterranean forecasting system eulerian velocity fields. *J. Geophys. Res.*, **112**(C05012).

Richardson, L. F., 1926: Atmospheric diffusion shown on a distance-neighbour graph. *Proceedings of the Royal Society A*, **110**, 709–737.

Rupolo, V., 2007: Observing turbulence regimes and lagrangian dispersal properties in the ocean. In *Lagrangian Analysis and Prediction of Coastal and Ocean Dynamics*, Griffa, A., Kirwan, A., Mariano, A., T.M., Ö., and Rossby, T., editors. Cambridge University Press.

Salazar, J. P. L. C. and L. R. Collins, 2009: Two-particle dispersion in isotropic turbulent flows. *Annual Reviews in Fluid Mechanics*, **41**, 405–432.

Skvortsov, A., M. Jamriska, and T. C. DuBois, 2010: Scaling laws of passive tracer dispersion in the turbulent surface layer. *Physical Review E*, **82(5):056304**.

Soomere, T., N. Delpeche, B. Viikmäe, E. Quak, H. E. M. Meier, and K. Döös, 2011: Patterns of current-induced transport in the surface layer of the gulf of finland. *Bor. Env. Res.*, **16A**, 49–63.

Soomere, T., K. Myrberg, M. Leppäranta, and A. Nekrasov, 2008: The progress in knowledge of physical oceanography of the gulf of finland: a review for 1997–2007. *Oceanologia*, **50**, 287–362.

Soomere, T., M. Viidebaum, and J. Kalda, 2011: On dispersion properties of surface motions in the gulf of finland. *Proceedings of the Estonian Academy of Sciences*, **60**(4), 269–279.

Table 1: The first transmitted positions ($\sim$ release positions) of all 12 surface drifters, and their duration.

Drifter	Initial Lon/Lat	Start date	Life-time
# 1	20.6984°E/58.3559°N	14 July 2010	96 days
# 2	20.6988°E/58.3562°N	14 July 2010	102 days
# 3	20.6967°E/58.3568°N	17 August 2010	317 days
# 4	20.6971°E/58.3567°N	17 August 2010	11 days
# 5	20.7002°E/58.3539°N	9 June 2011	22 days
# 6	20.6976°E/58.3532°N	9 June 2011	63 days
# 7	20.6987°E/58.3539°N	9 June 2011	25 days
# 8	19.8129°E/58.8452°N	10 August 2011	101 days
# 9	19.8128°E/58.8447°N	10 August 2011	100 days
# 10	19.8096°E/58.8462°N	10 August 2011	101 days
# 11	24.7421°E/59.6804°N	7 November 2011	12 days
# 12	24.7415°E/59.6796°N	7 November 2011	12 days

Soomere, T., B. Viikmäe, N. Delpeche, and K. Myrberg, 2010: Towards identification of areas of reduced risk in the gulf of finland, the baltic sea. *Proceedings of the Estonian Academy of Sciences*, **59**, 156–165.

Uppala, S. and co authors, 2005: The era-40 re-analysis. *Q. J. R. Meteorol. Soc.*, **131**, 2961–3012.

Vandenbulcke, L., J.-M. Beckers, F. Lenartz, A. Barth, P.-M. Poulain, M. Aidonidis, J. Meyrat, F. Ardhuin, M. Tonani, C. Fratianni, L. Torrisi, D. Pallela, J. Chiggiato, M. Tudor, J. W. Book, P. Martin, G. Peggion, and M. Rixen, 2009: Super-ensemble techniques: Application to surface drift prediction. *Progress in Oceanography*, **82**, 149–167.

Verjovkina, S., U. Raudsepp, T. Kõuts, and K. Vahter, 2010: Validation of seatrack web using surface drifters in the gulf of finland and baltic proper. In *2010 IEEE/OES US/EU-Baltic International Symposium, Riga, Latvia, August 25–27*, 7.

Webb, D. J., A. C. Coward, B. A. de Cuevas, and C. S. Gwilliam, 1997: A multiprocessor ocean general circulation model using message passing. *J. Atmos. Oceanic Technol.*, **14**(1), 175–183.

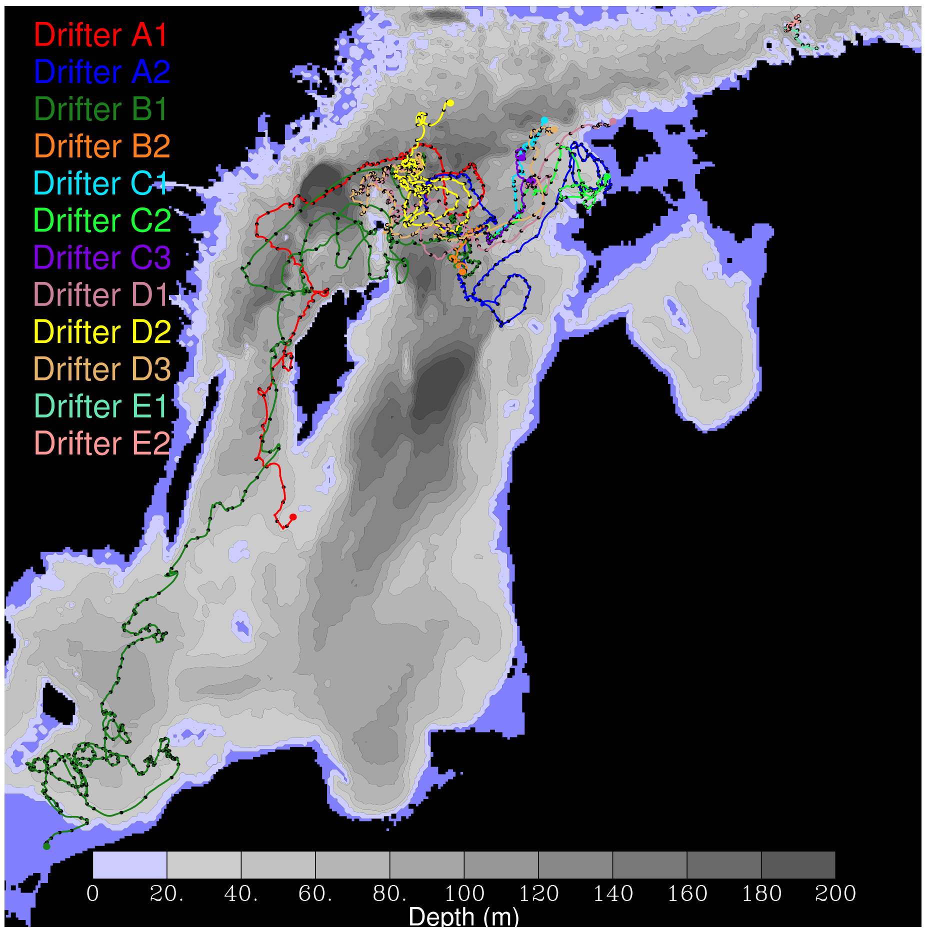

Figure 1: The 12 surface drifters used in this study mapped on top of the bathymetry. Depth < 20m is indicated by purple shading.

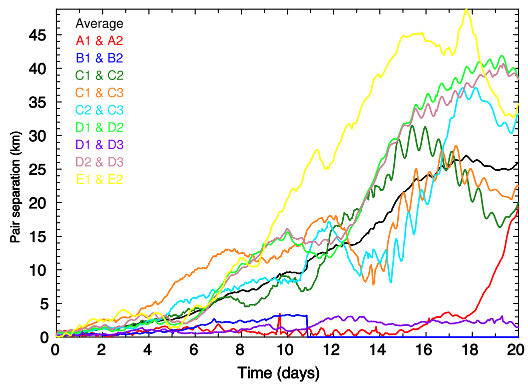

Figure 2: Pair separation for each individual drifter pair. The pair separation is related to the relative dispersion by a factor 2. Surface drifters are given a letter corresponding to the deployment event. A and B are the two pairs deployed in 2010, C and D the two triplets in 2011, and E is the pair deployed in 2011 in the Gulf of Finland.

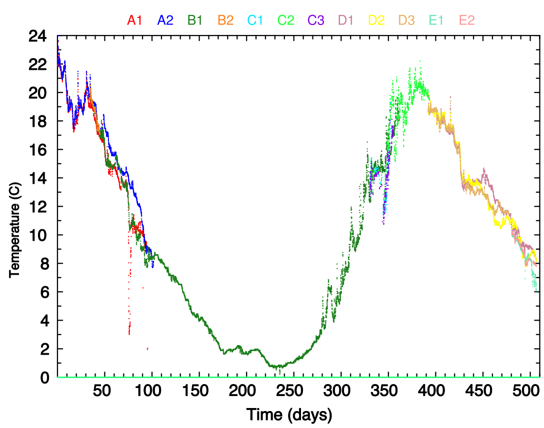

Figure 3: The sea-surface temperature (SST) measured by each drifter. Horizontal time axis is days from the first deployment, 14 July 2010, up to December 2011 when the data collection was stopped. The SSTs were constantly above 0°C indicating ice-free conditions.

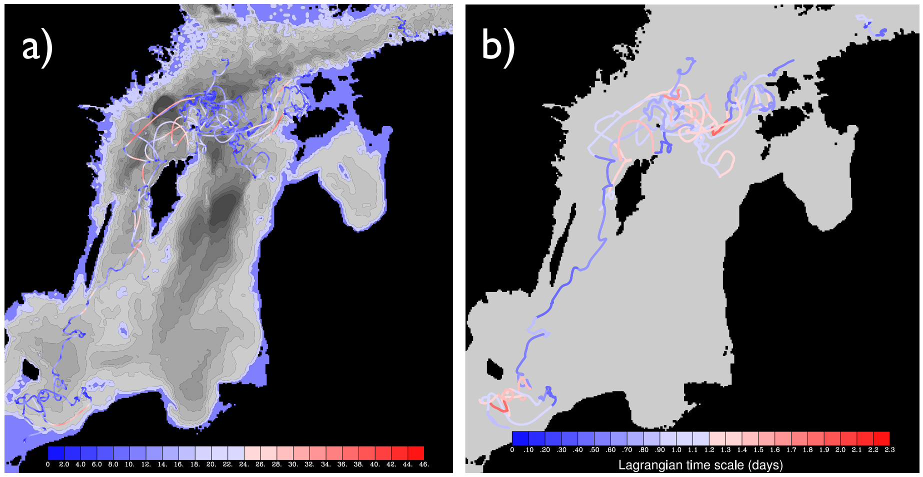

Figure 4: a) Surface drifter trajectories coloured by their total Lagrangian velocities. The colour range is from 0 to 0.45 ms^{-1}. Velocities are found especially strong near the coast of Poland/Bay of Gdansk, west coast of Gotland and east of Estonia. b) Surface drifter trajectories coloured by the Lagrangian integral time scales. Calculations of Lagrangian time scales yielded one value per drifter segment (256 hours). Colours range from 0 to 2.3 days. Short Lagrangian integral time scales are found near the east coast of Sweden, the west coast of Estonia, and the Gulf of Finland. Longer time scales are found near one of the deployment points (between Sweden and Estonia).

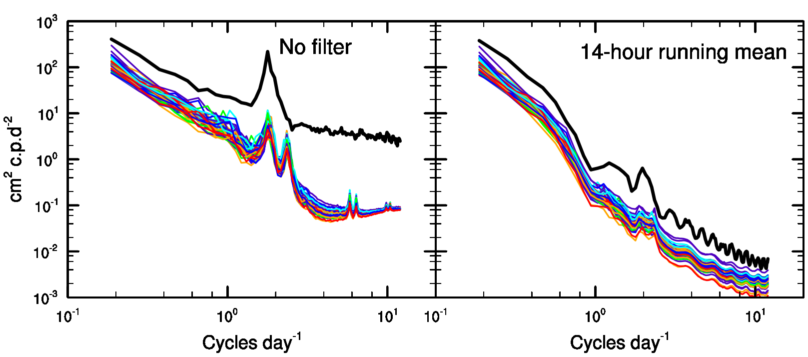

Figure 5: Power spectra of the Lagrangian velocity. Surface drifter data is shown as a thick black line, while each model year is shown as a thinner coloured line. Note the peak just below 2 cycles per day for the surface drifters which is less visible for the model trajectories (left figure). This frequency corresponds to a period of $\sim$ 14 hours, consistent with the theoretical calculations for inertial oscillations in the Baltic Sea. The right figure shows the power spectrum of the velocities when the inertial oscillations have been filtered out, which has been done for all data.

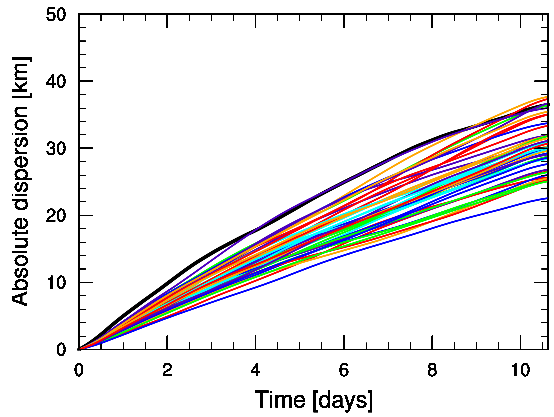

Figure 6: Mean absolute dispersion for segments of surface drifters deployed in 2010 and 2011 (thick black line), and for model trajectories during all model years (thin coloured lines). The mean absolute dispersion grows as a function of time, but shows signs to level off after 11 days. It is also lower for the model-simulated trajectories than for the surface drifter segments in most model years.

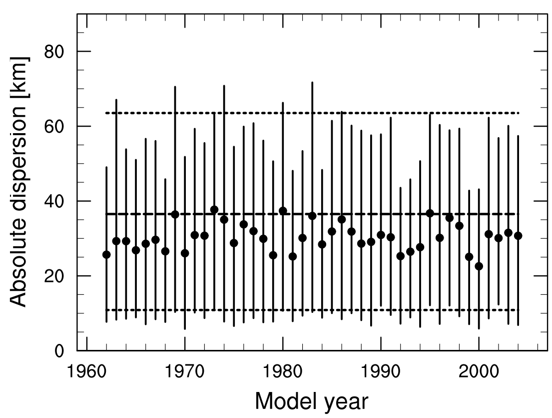

Figure 7: Mean absolute dispersion for each model run after 256 hours (black dots) and for the drifter segments (thick black dashed line). Also shown are the 90th and 10th percentiles for the model years (edges of vertical bars) and for the drifter segments (thin black dashed lines). As in Fig. 6, the mean absolute dispersion is lower for most model years than for the drifter data. It is also found that the 10th and 90th percentiles are lower for most model years than for the drifter data.

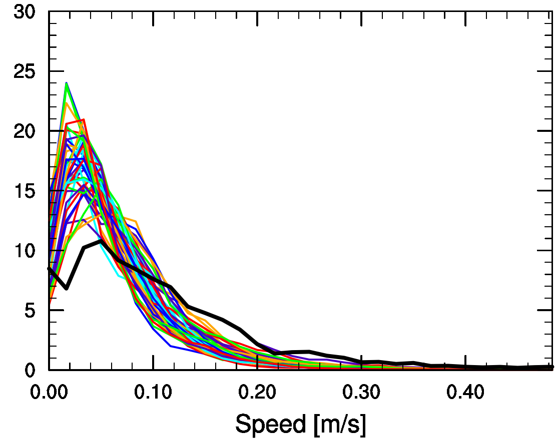

Figure 8: Distribution of the Lagrangian velocities (Eq. (3)) for surface drifter segments and model trajectories in all model years. Thick black line is surface drifter segments, and the thinner lines are model results from different years. The vertical axis is scaled such that the integral of any distribution is 1. Note how the distributions model-simulated velocities are narrower and displaced towards lower values that the distribution of drifter velocities.

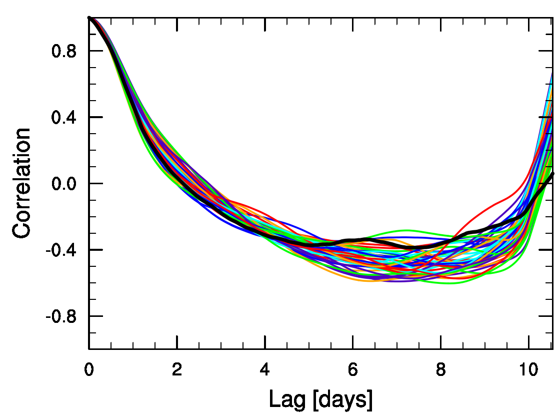

Figure 9: Mean Lagrangian velocity auto-correlation, $R(\tau)$, for drifter segments (thick black line) and for model trajectories in all model years (thin coloured lines). Horizontal axis is the time lag, τ, in days. Note that all trajectories, observed and modelled, were filtered using a 14-hour running mean. The smallest τ for which $R(\tau) = 0$ is the upper limit of the integral in Eq. (7).

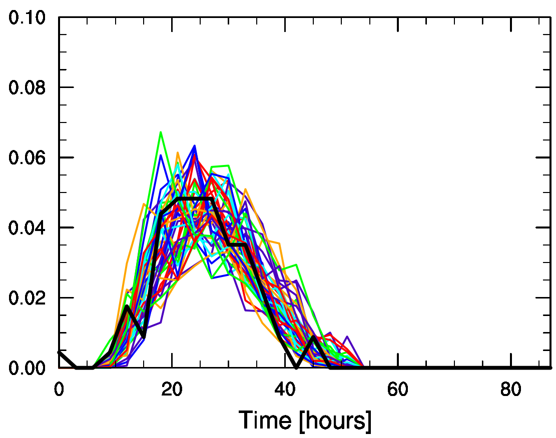

Figure 10: Distribution of the total Lagrangian integral time scales for the drifter segments (thick black line) and model-simulated trajectories (thin coloured lines) in all model years. Time scales are roughly normally distributed around a mean of ~ 1 day. Distributions are scaled such that the integral of any curve is 1.

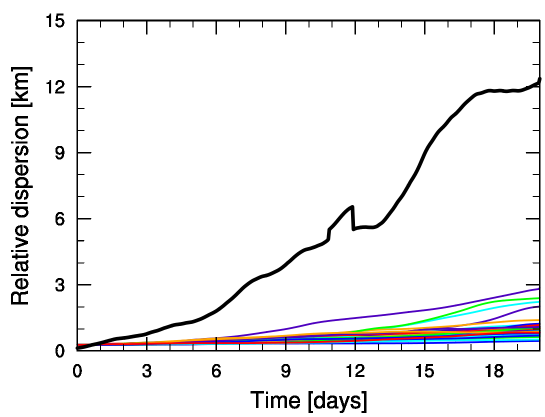

Figure 11: Mean relative dispersion of surface drifter pairs (thick black line), and corresponding pairs of model trajectories for each model year (thin coloured lines). The initial pair separation for both drifters and model trajectories is $O(100\text{m})$, well smaller than the grid box width. Mean relative dispersion is an order of magnitude higher for drifter pairs than for pairs of model trajectories.

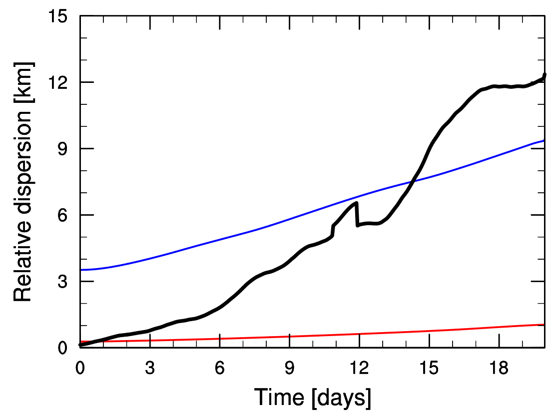

Figure 12: As Fig. 11, but an average is calculated of all model years (red line). The blue line shows the same average of model years, but with trajectory pairs initially separated by > 4km. This increased the relative dispersion by an order of magnitude.

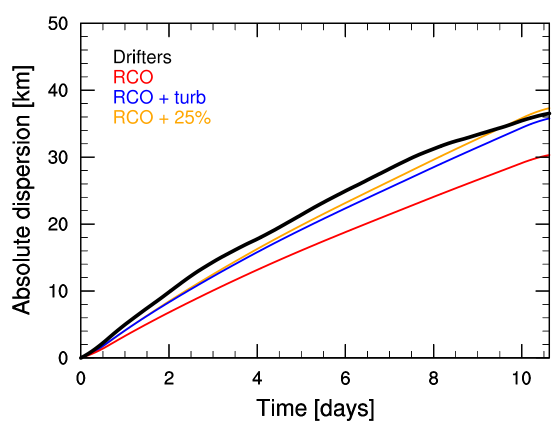

Figure 13: Mean absolute dispersion for surface drifter segments (black), and for all model-simulated trajectories in all model years (red). Also shown is the results when including parameterised sub-grid turbulence (green), and when multiplying the model-simulated velocity fields by 1.25 (blue).

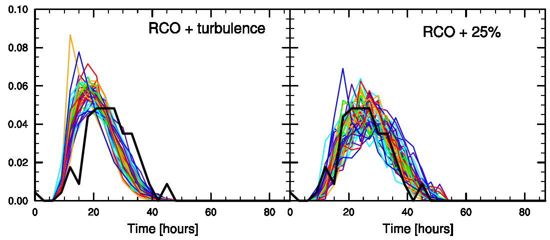

Figure 14: Distribution of the Lagrangian integral time scales for all drifter segments (thick black) and all model-simulated trajectories in each model year (thin coloured). Left panel shows for model simulations with added sub-grid turbulence of $A_H = 200$, and the right shows model simulations where the horizontal velocities at each point and time step are multiplied by 1.25. Turbulence parameterisation clearly shifts the distributions towards lower values. Vertical scale is such that the integral of any distribution is 1.

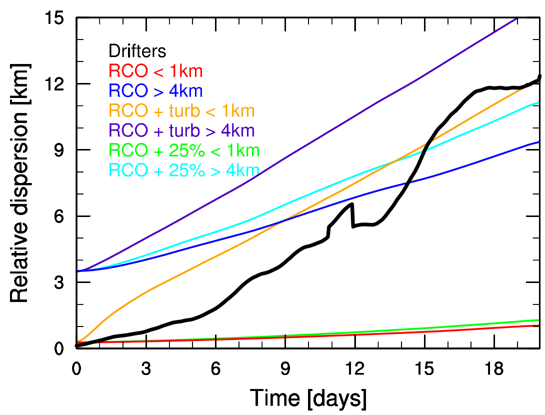

Figure 15: Mean relative dispersion for surface drifter segments (black), and for all model-simulated trajectories in all model years. As in Fig. 12, two sets of trajectories are shown for each simulation; those with initial pair separation < 1km (red, green, orange) and those with > 4km (blue, cyan, purple). The simulations shown are the original (red, blue), one with added sub-grid turbulence (orange, purple) and one where all model-simulated velocities were increased by 25% (green, cyan).

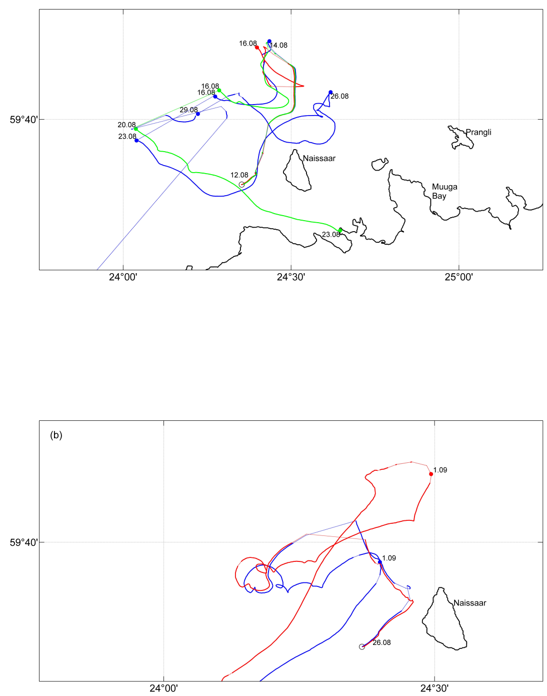

Figure 16: Trajectories of drifters deployed on 12.08.2010 (top panel) and on 26.08.2010 (bottom panel) in the Gulf of Finland. The deployment site is indicated by an empty circle. Thin straight sections of the trajectories represent intervals when the GSM signal was not available (Soomere et al., 2011).

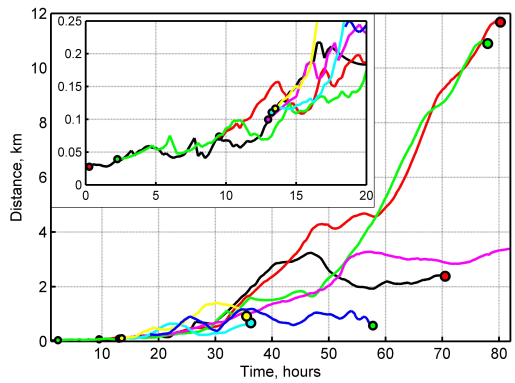

Figure 17: Temporal course of the distance between pairs in linear coordinates. Circles show the beginning and end of sensible measurements of the pairs locations. The beginning time is chosen so that the initial separation of each pair matches the average distance of pairs deployed with initially smaller separation. The insert shows the pairs separation during the first 20 hours (Soomere et al., 2011).

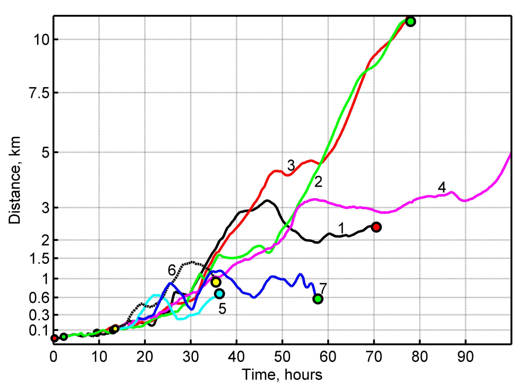

Figure 18: Temporal course of the distance between pairs of drifters in linear power law 2/3 coordinates (Soomere et al., 2011).

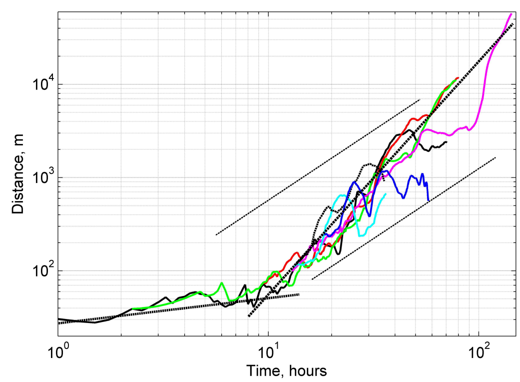

Figure 19: Temporal course of the distance between pairs of drifters in log-log coordinates. Bold dashed lines correspond to the power laws with $b = 0.27$ (time interval $1 - 10.5$ hours) and $b = 2.5$ (time interval $8 - 105$ hours). Dashed lines correspond to the Richardsons law with $b = 1.5$ (Soomere et al., 2011).